Heliyon 9 (2023) e21110

Contents lists available at ScienceDirect

Heliyon

journal homepage: www.cell.com/heliyon

Arenobufagin increases the sensitivity of gastric cancer to cisplatin via alkaliptosis

Chengwei Liu, Dongchang Li, Jian Wang, Zhengguang Wang *

Department of General Surgery, First Affiliated Hospital of Anhui Medical University, Hefei, Anhui, PR China

ARTICLE INFO

Keywords:
Arenobufagin
Cisplatin
Gastric cancer
Alkaliptosis

ABSTRACT

Background: Gastric cancer is the third leading cause of cancer-related death worldwide, for which several novel therapeutic strategies have been developed. Cisplatin (CDDP) mainly exerts its anti-gastric cancer effects; however, drug resistance limits its use. Thus, the development of drugs that can augment their antitumor effects is necessary. Arenobufagin (ArBu) is a novel anticancer drug, and the effects of ArBu in combination with CDDP on gastric cancer have not yet been studied.
Aims: To identify a possible synergistic effect between ArBu and CDDP in gastric cancer and investigate the underlying mechanism.
Methods: Cell viability, colony formation, migration, apoptosis, cell cycle, western blotting, immunofluorescence, and reverse-transcription polymerase chain reaction (RT-PCR) were analyzed in vitro. Western blotting, RT-PCR, hematoxylin and eosin (H&E) staining and blood biochemistry were carried out to examine in vivo.
Results: We found that ArBu, in combination with CDDP, effectively inhibited the proliferation and migration of gastric cancer cells, promoted apoptosis, and downregulated the expression of carbonic anhydrase 9 (CA9), matrix metalloproteinase-2 (MMP-2), and matrix metalloproteinase-9 (MMP-9). In addition, treatment with ArBu in combination with CDDP increased the level of inhibitor of nuclear factor kappa B kinase subunit beta (IKBKB), E-cadherin, and nuclear factor kappa-B/p65 (NF-κB/p65). Furthermore, the combination of ArBu and CDDP inhibited tumor growth in xenograft nude mice with no obvious side effects.
Conclusions: ArBu synergizes with CDDP to inhibit tumor growth both in vivo and in vitro by inducing alkaliptosis. This indicated that ArBu combined with CDDP may serve as a potential agent for the treatment of gastric cancer.

1. Introduction

According to the latest World Health Organization assessment, gastric cancer is the third leading cause of cancer-related deaths worldwide [1]. Gastric cancer generally carries a poor prognosis, because it is usually diagnosed at an advanced stage, despite tremendous developments in detection and treatment strategies [2,3]. Surgery may be a prospective cure, but the high incidence, recurrence rate, and drug resistance of gastric cancer make it impossible to improve its prognosis [4,5]. Therefore, developing therapeutic strategies to improve the prognosis and quality of life of these patients is imperative.

Cisplatin (*cis*-diamminedichloroplatinum, CDDP), a platinum-containing anticancer drug, is the first-line chemotherapy for gastric

* Corresponding author. Department of General Surgery, First Affiliated Hospital of Anhui Medical University, Hefei, 230032, Anhui, PR China.
E-mail address: wangzhengguang@ahmu.edu.cn (Z. Wang).

https://doi.org/10.1016/j.heliyon.2023.e21110
Received 28 July 2023; Received in revised form 14 October 2023; Accepted 16 October 2023
Available online 19 October 2023

cancer [6,7]. A previous study has shown that the anticancer effect of CDDP depends on its ability to generate irreparable DNA lesions [8]. However, the clinical responses elicited by CDDP in patients usually disappear owing to resistance to its cytotoxic activity and toxic side effects [6,9]. Therefore, new drugs are required to reverse the acquired drug resistance and improve survival and quality of life. Previous studies have shown that several toad venoms could achieve this goal [10,11].

Arenobufagin (ArBu), the main active ingredient of toad postauricular and skin gland secretions, or dry skin extracts of *Bufo gargarizans* and *Duttaphrynus melanostictus*, has been shown to exert antitumor effects by promoting apoptosis and inhibiting invasion, metastasis, and angiogenesis in various types of cancer [12–14]. ArBu induces apoptosis and autophagy in hepatocellular carcinoma cells through the phosphatidylinositol 3-kinase (PI3K)/protein kinase B (Akt)/mammalian target of rapamycin (mTOR) signaling pathway, thereby exerting anti-hepatocellular carcinoma effect [15]. Additionally, Deng et al. found that ArBu plays a role in cell cycle arrest through the ataxia-telangiectasia-mutated (ATM) and ataxia telangiectasia and Rad3-related (ATR) signaling pathways, thereby promoting apoptosis in lung cancer PC-9 cells [16]. In summary, the above studies showed that ArBu has potential applications as a drug therapy for cancer treatment. However, whether ArBu enhances the efficacy of chemotherapy in gastric cancer remains unclear. In this study, we investigated the synergistic effects of ArBu in combination with CDDP on anticancer activity in AGS and MKN-45 cells and in a mouse xenograft model.

The main goal of cancer therapy is to inhibit the biological capabilities of tumors, and most chemotherapeutic drugs rely on the induction of cell death for efficacy. Alkaliptosis, a type of regulatory cell death, is a non-apoptotic programmed cell death process [17]. Alkaliptosis, depending on the activation of nuclear factor kappa-B/p65 (NF-κB/p65) and down-regulation of carbonic anhydrase 9 (CA9) expression, has become a drug target for a variety of cancers [18]. Furthermore, patients with higher expression of CA9 in gastric cancer specimens had a poorer prognosis than those with lower expression [19]. CA9 inhibitors combined with CDDP chemotherapy have been shown to significantly enhance apoptosis and inhibit tumor growth in small cell lung cancer [20,21].

Overall, these studies demonstrate that the molecular mechanism of alkaliptosis might also be involved in the suppression of gastric cancer. However, studies on the anticancer effects and mechanisms of action of ArBu in gastric cancer cells are rare. Here, we hypothesized that the combination of ArBu and CDDP would inhibit gastric cancer via alkaliptosis. To test this hypothesis, we used human gastric cancer cells and a tumor xenograft mouse model, determined the effects of CDDP, ArBu, and ArBu in combination with CDDP on gastric cancer growth, and explored the underlying molecular mechanisms.

2. Materials and methods

2.1. Chemical and reagents

CDDP was purchased from MedChemExpress (MCE, New Jersey, USA). ArBu, with a molecular formula of $C_{24}H_{32}O_6$ and a molecular weight of 416.51 was purchased from MedChemExpress (MCE, New Jersey, USA). The Cell Counting Kit-8 (CCK-8) assay kit was purchased from MedChemExpress (MCE, New Jersey, USA). Dimethyl sulfoxide (DMSO) was procured from Good Laboratory Practice Bioscience (GLPBIO, Montclair, California, USA). The bicinchoninic Acid (BCA) protein assay kits were obtained from Beyotime (Shanghai, China). The Annexin V fluorescein-isothiocyanate (AV-FITC)/propidium iodide (PI) apoptosis detection kit was purchased from Beyotime (Shanghai, China). Primary antibodies against CA9, inhibitor of nuclear factor kappa B kinase subunit beta (IKBKB), NF-κB, matrix metalloproteinase-2 (MMP-2), matrix metalloproteinase-9 (MMP-9), E-cadherin, and GAPDH were purchased from Affinity Biosciences (Cincinnati, OH, USA). The anti-rabbit, IgG, anti-mouse IgG, and HRP-conjugated antibodies were purchased from Beyotime (Shanghai, China). Enhanced chemiluminescence (ECL) kits were purchased from Affinity Biosciences (Cincinnati, OH, USA).

2.2. Cell culture and treatments

Human gastric cancer cell lines AGS and MKN-45 were obtained from the Shanghai Institutes for Biological Sciences, Chinese Academy of Sciences (Shanghai, China). AGS and MKN-45 cells were cultured in RPMI-1640 and DMEM (high glucose), respectively, supplemented with 10 % heat-inactivated fetal bovine serum (FBS) and antibiotics (100 U/ml of penicillin and 100 μg/ml of streptomycin; Wako Pure Chemical Industries) in a humidified 5 % CO_2 atmosphere at 37 °C.

2.3. Cell viability evaluation

Cells were seeded in a 6-well plate at a density of 1×10^6 cells/2 ml media, which were treated with ArBu (10, 20, 40, 60, and 80 nM), CDDP (10, 20, 40, 60, and 80 μM). Following treatment for 12, 24, and 48 h, cell viability was measured using a CCK-8 kit. The cells were seeded in a 96-well plate at a density of 1×10^5 cells/well. After treatments, CCK-8 solution (10 μl) was added to each well of the plate, which was then incubated for 1 h. Optical density of each well was determined by using a microplate reader at 450 nm. Relative cell viability is expressed as the ratio of the absorbance of each treatment group to that of the corresponding untreated control group. The ED50 values of the drugs were calculated using GraphPad Prism 8 software.

2.4. Wound healing assay

AGS and MKN-45 cells were cultured in 6-well plates (3×10^5 cells/well). When AGS and MKN-45 cells reached approximately 90–95 % confluence, the monolayer was scratched with a 200 μl pipette tip at the time recorded as 0 h. Then the cells were treated with

control (DMSO), ArBu (40 nM), CDDP (40 μM), ArBu combination with CDDP (24.61 nM plus 28.37 μM) for 12 and 24 h. The culture medium was removed and the plate was washed three times with phosphate-buffered saline (PBS) three times. Cell debris produced during scratching was washed away, followed by the addition of serum-free culture medium and imaging at 12 and 24 h. ImageJ software (Bethesda, MD, USA) was used to calculate the migration distances.

2.5. Colony formation assay

AGS and MKN-45 cells were resuspended in complete medium containing 10 % FBS. A total of 1.5×10^3 treated cells were coated into 6-well plates in triplicate. Cells were inoculated into dishes containing concentrations of control (DMSO), ArBu (40 nM), CDDP (40 μM) and ArBu combination with CDDP (24.61 nM plus 28.37 μM) culture solution for 24 h. After treatment, the cells were allowed to form colonies for 14 days. After 14 days of incubation, the plates were washed twice with PBS, fixed with methanol for 10 min, stained with 0.1 % crystal violet solution, and within 10 min visualized under a dissection microscope (Olympus, Tokyo, Japan). Clone formation rate was calculated as follows: clone formation rate = number of clones/number of inoculated cells × 100.

2.6. Apoptosis assay

AGS and MKN-45 cells were cultured overnight in 6-well plates (3×10^5 cells per well) and then separately treated with control (DMSO), ArBu (40 nM), CDDP (40 μM), ArBu combination with CDDP (24.61 nM plus 28.37 μM) for 24 h. Apoptosis ratios of AGS and MKN-45 cells were measured using AV and PI apoptosis detection kit Beyotime (Shanghai, China) by flow cytometry. After stimulation, the cells were washed with PBS and incubated with 10 μL of AV-FITC and 5 μL of PI for 15 min at room temperature in the dark. Flow cytometry was performed using a FACScan flow cytometer (Beckman Coulter, Fullerton, CA, USA), and the data were analyzed by using FlowJo software (Tree Star, Ashland, OR, USA).

2.7. Cell cycle analysis

Cell cycle analysis was performed using flow cytometry (FACS LSR II, BD Bioscience, USA) according to the manufacturer's protocol. AGS and MKN-45 cells were separately treated with control (DMSO), ArBu (40 nM), CDDP (40 μM), ArBu combination with CDDP (24.61 nM plus 28.37 μM) for 24 h. Treated cells were collected and fixed with chilled 75 % ethanol at −20 °C overnight. After ethanol was discarded, cells were washed twice with PBS and resuspended with 250 μl DNA staining solution (MultiSciences, China) at room temperature for 30 min.

2.8. Immunofluorescence

AGS cells were seeded into 24-well plates at a density of approximately 5×10^4 cells/well and cultured overnight, followed by treatment with control (DMSO), ArBu (40 nM), CDDP (40 μM), ArBu combination with CDDP (24.61 nM plus 28.37 μM) for 24 h. Cells were fixed with 4 % paraformaldehyde and permeabilized with 0.1 % Triton X-100 in PBS. Following cell fixation, cells were incubated with the appropriate primary antibodies CA9, IKBKB, NF-κB (Proteintech, Chicago, USA) in a solution of PBS with 1 % bovine serum albumin at 4 °C overnight. The cells were then incubated with FITC (HY-66019; MCE, New Jersey, USA) labeled with secondary antibodies for 1 h at room temperature. Nuclei were stained with DAPI for 5 min. Fluorescence signals were detected by confocal fluorescence microscopy.

2.9. RT-PCR

AGS and MKN-45 cells were seeded in 6 cm culture capsules and treated with control (DMSO), ArBu (40 nM), CDDP (40 μM), ArBu

Table 1
Sequences of primers used for human cells in the real-time PCR.

Gene	Sequence (5′-3′) Primer Sequence
GAPDH	Forward CAAGAGCACAAGAGGAAGAGAG
	Reverse CTACATGGCAACTGTGAGGAG
MMP-2	Forward GATAACCTGGATGCCGTCGTG
	Reverse GGTGTGCAGCGATGAAGATGATA
MMP-9	Forward CATCCGTAAAGACCTCTATCCCAAC
	Reverse ATGGAGCCACCGATCCACA
CA9	Forward GCCTTTGAATGGGCGAGTG
	Reverse CCTTCTGTGCTGCCTTCTCATC -
NF-κB/p65	Forward TCCACTGTCTGCCTCTCTCGTC
	Reverse GCCTTCAATAGGTCCTTCCTGC
IKBKB	Forward GTCTTTGCACATCATTCGTGGG
	Reverse GTGCCGAAGCTCCAGTAGTC
E-cadherin	Forward CGGGAATGCAGTTGAGGATC
	Reverse AGGATGGTGTAAGCGATGGC

combination with CDDP (24.61 nM plus 28.37 μM). After 48 h of incubation, the cells were collected and total RNA was extracted with TRIzol reagent. Total RNA was isolated from the tumorigenic tissues of nude mice using TRIzol reagent (Invitrogen) according to the manufacturer's instructions. Reverse transcription was performed using a MultiScribe RT kit (Applied Biosystems, Foster City, CA, USA). For analysis of CA9, NF-κB, IKBKB, MMP-2, MMP-9, and E-cadherin, the SYBR Green PCR kit (TaKaRa, Japan) was used to quantify the messenger RNA (mRNA) levels. GAPDH was used as a control and relative expression levels of CA9, NF-κB, IKBKB, MMP-2, MMP-9, and E-cadherin were calculated using the $2^{-\Delta\Delta}$CT method. The primer sequences for these genes in human cells and nude mice are listed in Tables 1 and 2, respectively. All experiments were performed independently and in triplicates.

2.10. Western blotting assay

AGS and MKN-45 cells (1×10^7) were treated with control (DMSO), ArBu (40 nM), CDDP (40 μM), ArBu combination with CDDP (24.61 nM plus 28.37 μM) for 48 h to evaluate changes in alkaliptosis-related protein levels. AGS and MKN-45 cells and tumorigenic tissues of nude mice were lysed using RIPA lysis buffer (Beyotime Biotechnology, Shanghai, China) and proteins were quantified using a BCA protein assay kit (Beyotime. Shanghai, China). Equal amounts of protein were separated by sodium dodecyl sulfate-polyacrylamide gel electrophoresis and transferred onto polyvinylidene fluoride membranes (GLPBIO, Montclair, California, USA). Membranes were incubated with the indicated primary and secondary antibodies. The primary antibodies used in this study included anti-CA9 (11071-1-AP, 1:1000, Proteintech, Chicago, USA), anti–NF–κB (10745-1-AP, 1:1000, Proteintech, Chicago, USA), anti-IKBKB (15649-1-AP, 1:1000, Proteintech, Chicago, USA), anti-MMP-2 (AF5330, 1:2000, Affinity Biosciences, Boston, USA), anti-MMP-9 (AF5228, 1:2000, Affinity Biosciences, Boston, USA), anti-E-cadherin (AF0131, 1:2000, Affinity Biosciences, Boston, USA) and GAPDH (AF7021, 1:1000, Affinity Biosciences, Boston, USA) was used as the loading control. Immunoreactive bands were visualized using ECL detection reagent (Affinity Biosciences). The intensity of the bands was quantified using ImageLab Software (Bio-Rad, California, USA).

2.11. Mouse xenograft model and treatments

The mouse experiments were approved by the Institutional Animal Care and Use Committee of the First Affiliated Hospital of Anhui Medical University (Approval Number: LLSC20180365) in accordance with the Guide for the Care and Use of Laboratory Animals. All male mice were fed in a pathogen-free environment with well-controlled temperature (20–24 °C) and humidity (40–60 %). A total of 1×10^7 AGS cells were injected subcutaneously into the right axilla of nude mice. When the tumors reached a size of approximately 200 mm^3 after approximately 24 days, 20 mice were randomly divided into four groups with five mice in each group. Treatments in each group were shown as follows: control (0.1 % DMSO solvent), ArBu (6.4 mg/kg) [22], CDDP (3 mg/kg) [23] and ArBu combination with CDDP (6.4 mg/kg plus 3 mg/kg). All mice were intraperitoneally administered the drugs three times a week for 3 weeks. The tumors and body weights of the nude mice were monitored daily. At the end of the experiment, the mice were euthanized. The tumors were removed for imaging purposes.

2.12. H&E staining

The hearts, livers, and kidneys were rinsed with cold saline and fixed in 4 % paraformaldehyde. Paraffinized tissues were dehydrated in gradient proportions of ethyl alcohol and embedded in paraffin. After that, the tissues sections of 4 μm thickness were prepared and stained with H&E routinely.

2.13. Blood biochemistry

Serum creatinine and blood urea nitrogen (BUN) were measured using commercial kits (Jiancheng Bioengineering Institute,

Table 2
Sequences of primers used for mouse tissues in the real-time PCR.

Gene	Sequence (5′-3′) Primer Sequence
GAPDH	Forward GGTGAAGGTCGGTGTGAACG
	Reverse CTCGCTCCTGGAAGATGGTG
MMP-2	Forward ACCTGAACACTTTCTATGGCTG
	Reverse CTTCCGCATGGTCTCGATG
MMP-9	Forward GCAGAGGCATACTTGTACCG
	Reverse TGATGTTATGATGGTCCCACTTG
CA9	Forward CCGGAACTGAGCCTATCCAAC
	Reverse GCAAGGCCCGGTATTCCTG -
NF-κB/p65	Forward ATGGCAGACGATGATCCCTAC
	Reverse CGGAATCGAAATCCCCTCTGTT
IKBKB	Forward ATCAGGCGACAGGTGAACAG
	Reverse GGCCACAGCAGTTCTCGAA
E-cadherin	Forward CTCCAGTCATAGGGAGCTGTC
	Reverse TCTTCTGAGACCTGGGTACAC

Nanjing, China). Measurements were performed using a fluorescence spectrophotometer (SpectraMax; Molecular Devices, Sunnyvale, CA, USA) according to the manufacturer's instructions.

2.14. Statistical analysis

Data from this study are presented as mean ± standard deviation (SD) and statistically analyzed by one-way analysis of variance (ANOVA) using SPSS (version 23.0; IBM Analytics, New York, USA). The difference between the theoretical ED50 and experimental ED50 was examined using Student's t-test. Statistical significance was set at $P < 0.05$. All experiments were repeated at least three times.

3. Results

3.1. ArBu increased the activity of CDDP to inhibit the viability of gastric cancer cells and impair migration and colony formation

The effects of ArBu and CDDP on the viability of AGS and MKN-45 cells were examined using a CCK-8 assay. Cells were exposed to increasing concentrations of ArBu (10, 20, 40, 60, and 80 nM) and CDDP (10, 20, 40, 60, and 80 μM) for different periods of time (12, 24, and 48 h). As shown in Fig. 1a, ArBu and CDDP reduced the viability of AGS and MKN-45 cells in a dose- and time-dependent manner. In AGS cells, dose for 50 % of maximal effect (ED50) values of ArBu and CDDP were 36.29 nM and 48.79 μM, respectively, after treatment for 24 h. In MKN-45 cells, the ED50 values of ArBu and CDDP were 48.11 nM and 38.28 μM, respectively, after treatment for 24 h (Fig. 1b). Using isobolographic analysis, the combination of ArBu ED50 and CDDP ED50 was 24.61 nM and 28.37 μM. The ED50 of the combination group was lower than that of the single drug groups (95 % confidence interval) (Fig. 1c). The ED50 of ArBu and CDDP in AGS and MKN-45 cells were approximately 40 nM and 40 μM. Therefore, we used these concentrations in subsequent experiments.

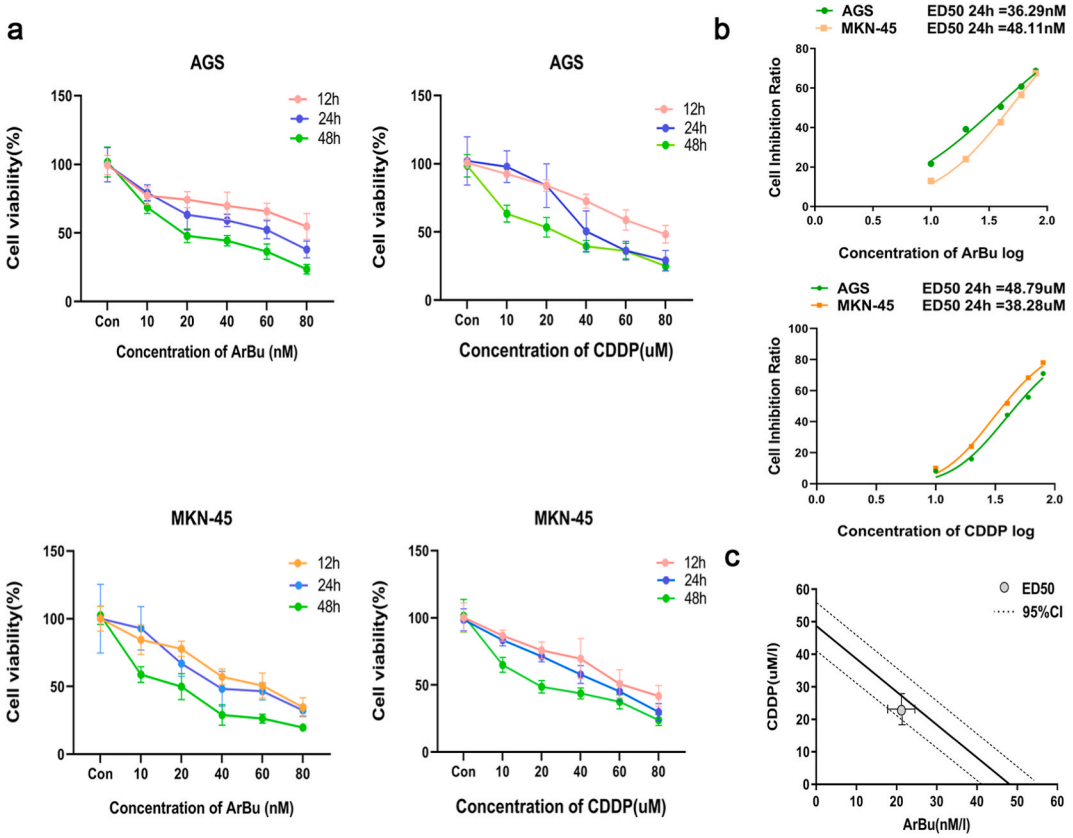

Fig. 1. ArBu and CDDP inhibit the viability of gastric cancer cells, as measured by the CCK-8 assay (a) The cytotoxic effects of the ArBu combination with CDDP on AGS and MKN-45 cells were examined using the CCK-8 assay. Cells were treated with different concentrations of ArBu (10, 20, 40, 60, and 80 nM) and CDDP (10, 20, 40, 60, and 80 μM) for 12, 24, and 48 h. (b) ED50 values were obtained after the two kinds of cells were treated with different concentrations of ArBu (10, 20, 40, 60, and 80 nM) and CDDP (10, 20, 40, 60, and 80 μM). (c) Isobolographic analysis of drug combination concentration. The data were presented as the mean (SD) of three independent experiments. $^{*}P < 0.05$ and $^{**}P < 0.01$, significantly different compared with the control treatment.

Furthermore, we observed that AGS and MKN-45 cells treated with ArBu in combination with CDDP had lower colony-forming ability than the single drug group cells (Fig. 2a). Next, we investigated whether ArBu in combination with CDDP inhibited the migration of cells. Then we found that ArBu combination with CDDP inhibited the migration of AGS and MKN-45 cells compared to ArBu (40 nM) or CDDP (40 μM) treatment in 12 h. As shown in Fig. 2b, the migration rate of the treated cells in the ArBu combination with CDDP group was lower than that in the ArBu or CDDP groups alone over a longer period of treatment (24 h) (Fig. 2b). These results indicated that the combination of ArBu and CDDP effectively inhibited the characteristics of gastric cancer, including viability, migration, and colony formation. The interaction between ArBu and CDDP showed a synergistic relationship and the combination of ArBu and CDDP may reduce the resistance of CDDP.

3.2. *ArBu increased the activity of CDDP to induce apoptosis and cell cycle arrest*

To determine the ability of the combination regimen and single treatment group to induce apoptosis. We treated AGS and MKN-45 cells with doses of ArBu (40 nM), CDDP (40 μM), ArBu combination with CDDP (24.61 nM plus 28.37 μM) for 24 h. The cells were then stained with AV-FITC/PI using flow cytometry to detect apoptosis. As shown in Fig. 3, the percentage of apoptotic cells in the control, ArBu and CDDP treated groups was 8.5 ± 3.23 %, 15.3 ± 1.38 %, and 13.8 ± 2.02 % in AGS cells and 7.7 ± 2.73 %, 16.8 ± 1.85 %, and 14.5 ± 4.32 % in MKN-45 cells, respectively, after 24 h of treatment. The apoptosis rate further increased to 23.47 ± 1.61 % and 26.1 ± 1.29 % in the ArBu combination with CDDP group in AGS and MKN-45 cells, respectively (Fig. 3a & b). Additionally, cell cycle analysis was performed after treatment with ArBu and CDDP for 24 h. PI staining and flow cytometry showed that ArBu, CDDP, and the

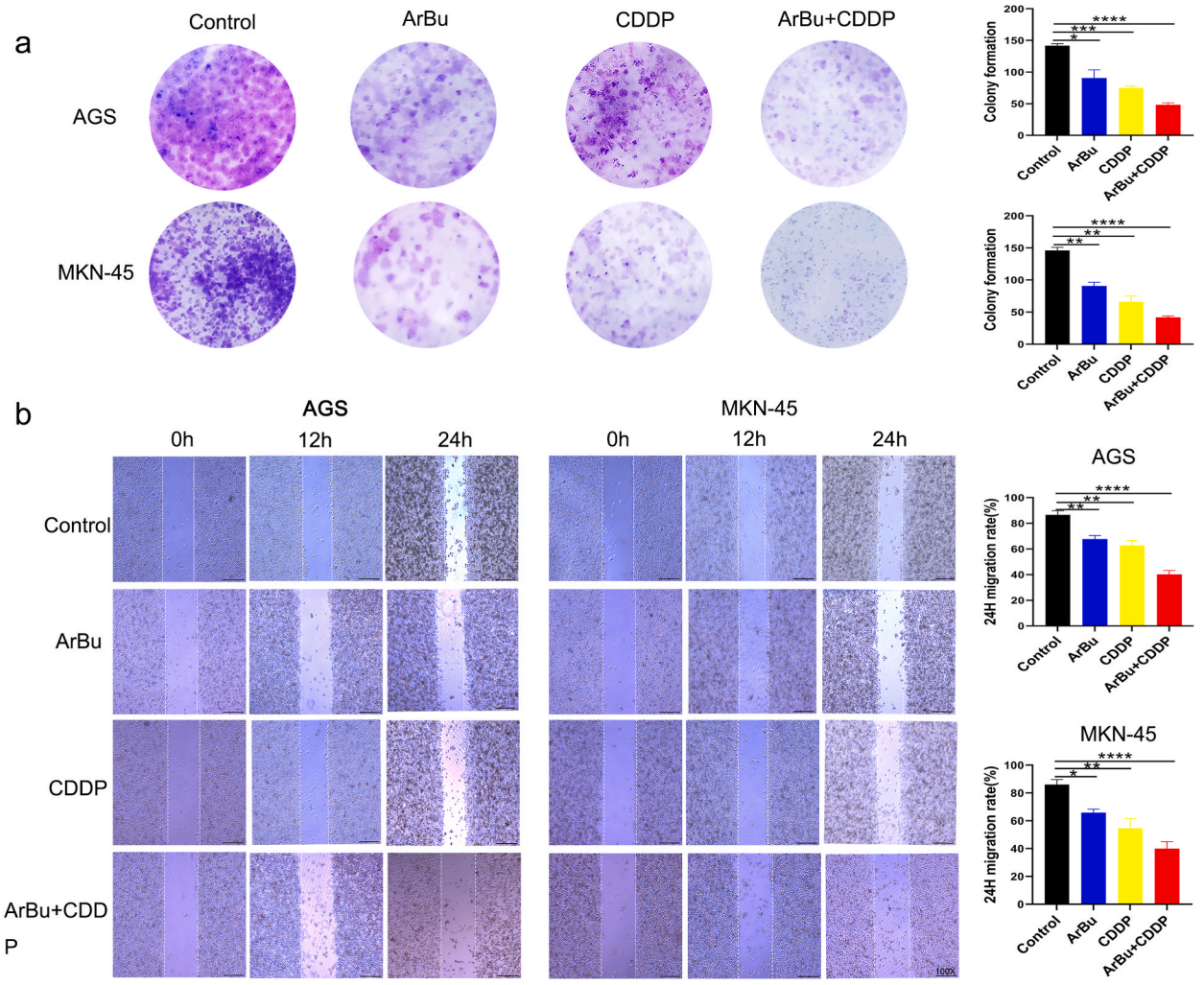

Fig. 2. The effect of the ArBu combination with CDDP on the proliferation and migration of gastric cancer cells (a) The colony formation assay was performed to indicate the proliferation of AGS and MKN-45 cells. (b) The migrations of AGS and MKN-45 cells were determined using scratch wound assay. Images were representative results of 3 independent experiments (100X). The data were presented as the mean (SD) of three independent experiments. *$P < 0.05$ and **$P < 0.01$, significantly different compared with the control treatment.

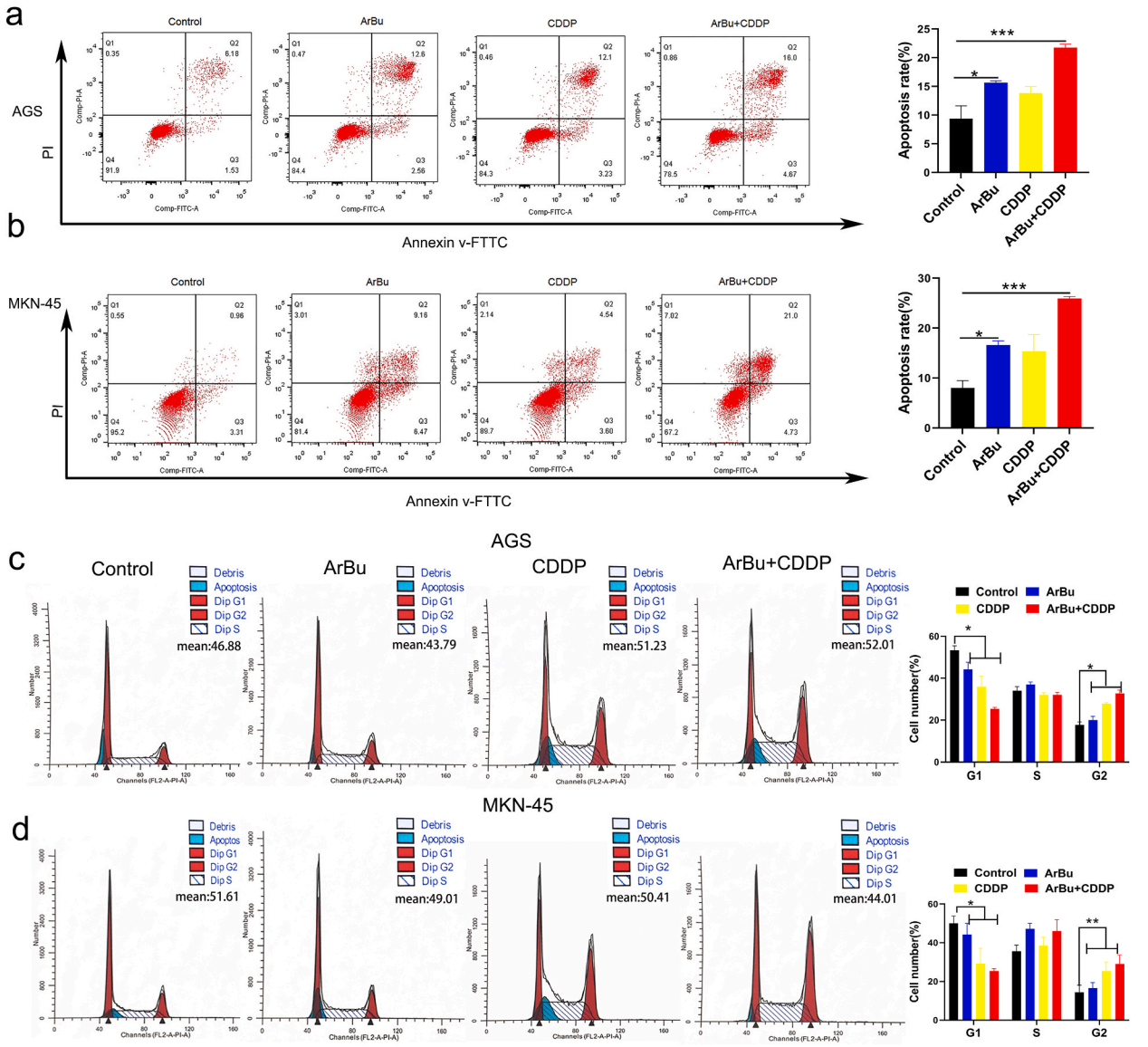

Fig. 3. The combination of ArBu and CDDP induces apoptosis and affects the cell cycle distribution of human gastric cancer cells (a, b) AGS and MKN-45 cells were separately treated with the control group, ArBu group (40 nM), CDDP group (40 μM), and ArBu combination with CDDP group (24.61 nM plus 28.37 μM) for 24 h. The effect of the ArBu combination with CDDP on apoptosis was also analyzed. (c, d) The cell cycle distribution was determined using flow cytometry analysis, and the cell cycle distribution was quantified. The data were presented as the mean (SD) of three independent experiments. $^{*}P < 0.05$ and $^{**}P < 0.01$, significantly different compared with the control treatment.

drug combination decreased the proportion of G0/G1 cells but increased the proportion of G2/M phase cells in AGS and MKN-45 cells compared to the control group. Moreover, the combination of ArBu and CDDP significantly enhanced the observed cell cycle change compared with the ArBu, CDDP, or control group, which is noteworthy (Fig. 3c & d).

3.3. ArBu increased the activity of CDDP to activate alkaliptosis pathway

The effect of ArBu combined with CDDP on alkaliptosis was demonstrated using various methods in AGS and MKN-45 cells. First, we detected the expression of alkaliptosis-related proteins using western blotting. Compared to the control, the ArBu and CDDP single treatment groups increased levels of IKBKB and NF-κB/p65 but decreased levels of CA9 in the AGS and MKN-45 cells. And the combination of ArBu and CDDP further decreased the level of CA9 and increased the levels of IKBKB and NF-κB/p65 than the ArBu or CDDP groups. Along with the activation of the alkaliptosis pathway, we found that the ArBu in combination with CDDP treatment downregulated the expression of invasion-associated proteins MMP-2 and MMP-9, but upregulated the expression of E-cadherin, compared to the ArBu or CDDP groups (Fig. 4a–d). Similar changes were observed at the mRNA level in AGS and MKN-45 cells

(Fig. 4e–f). Furthermore, subcellular localization of CA9, IKBKB, and NF-κB/p65 in AGS and MKN-45 cells treated with ArBu (40 nM), CDDP (40 μM), or ArBu combination with CDDP (24.61 nM plus 28.37 μM) were assessed using immunofluorescence. As shown in Fig. 5, the ArBu combination with CDDP remarkably reduced the translocation of CA9 from the cytoplasm to the nucleus and increased the translocation of IKBKB and NF-κB/p65 from the cytoplasm into the nucleus in AGS and MKN-45 cells, compared to the control, ArBu, and CDDP groups (Fig. 5a–c). These results suggest that the combination of ArBu and CDDP activated the alkaliptosis pathway.

3.4. ArBu increased the activity of CDDP to inhibit the growth of AGS xenografts in nude mice

The in vivo activity of ArBu combined with CDDP was demonstrated in a subcutaneous tumor xenograft mouse model of AGS cells. The cells were subcutaneously injected into BALB/c nude mice (5 per group) in vivo. After 24 days of intraperitoneal administration of the vehicle control (0.1 % DMSO solvent), ArBu (6.4 mg/kg), CDDP (3 mg/kg), or ArBu in combination with CDDP, tumor volumes and weights were measured. As shown in Fig. 6a, treatment with ArBu and CDDP inhibited tumor growth. Growth was further inhibited by treatment with the combination of ArBu and CDDP (Fig. 6b–c). However, there was no difference in the weights of the mice among the four groups (Fig. 6d). Next, we measured the expression of alkaliptosis-related proteins in these mice. Compared to the control group, ArBu or CDDP treatment increased levels of IKBKB and NF-κB/p65 but decreased CA9 levels. In addition, the invasion-associated proteins MMP-2 and MMP-9 were downregulated, whereas the expression of E-cadherin was upregulated by ArBu or CDDP treatment alone. Interestingly, we observed that the alkaliptosis pathway was further activated by the combination of ArBu and CDDP (Fig. 7a–b). This was confirmed by the mRNA expression of these proteins (Fig. 7c). These results suggested that ArBu and CDDP alone inhibited the growth of AGS xenografts in nude mice, which was associated with the activation of alkaliptosis. These effects were further augmented by the combination of ArBu and CDDP. Next, we determined the possible toxicity of ArBu, CDDP, and the combination of ArBu and CDDP in vital tissues. H&E staining revealed no edema, vacuole-like denaturation, structural derangement, local inflammation, or hemorrhage in the pathological sections of the heart, liver, and kidney among the different groups (Fig. 8a). Furthermore, there was no difference in serum creatinine and BUN levels between the groups. These results showed that ArBu combined with CDDP inhibited xenograft tumor growth without significant toxicity towards several important organs, which supports its potential for further clinical investigation in gastric cancer treatment (Fig. 8b).

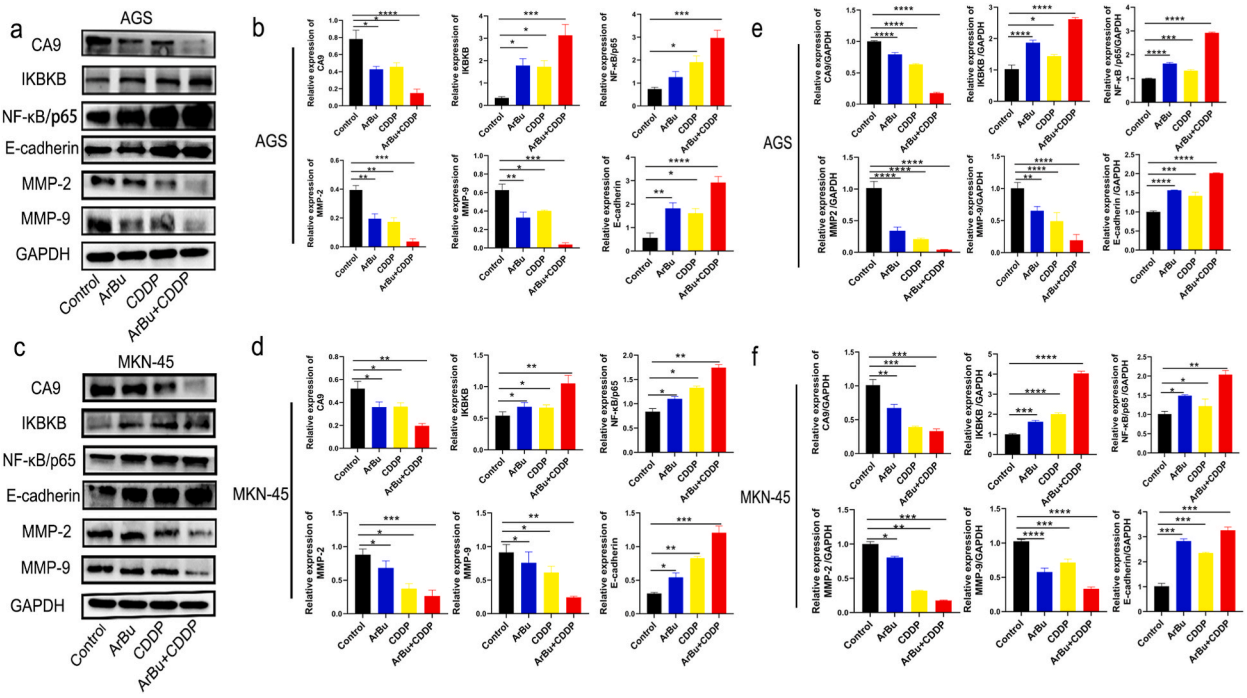

Fig. 4. The combination of ArBu and CDDP regulates the alkaliptosis pathway in vitro (a, b) The protein expression of CA9, IKBKB, NF-κB/p65, MMP-2, MMP-9, E-cadherin, and GAPDH in AGS cells was estimated by western blotting. (c, d) The protein expression of CA9, IKBKB, NF-κB/p65, MMP-2, MMP-9, E-cadherin, and GAPDH in MKN-45 cells was estimated by western blotting. (e, f) The mRNA expression of CA9, IKBKB, NF-κB/p65, MMP-2, MMP-9, and E-cadherin in AGS and MKN-45 cells treated with the control group, ArBu group (40 nM), CDDP group (40 μM), and ArBu combination with CDDP group (24.61 nM plus 28.37 μM). After treatment for 24 h, the mRNA level was detected by RT-PCR analysis. The data were presented as the mean (SD) of three independent experiments. $^{*}P < 0.05$ and $^{**}P < 0.01$, significantly different compared with the control treatment.

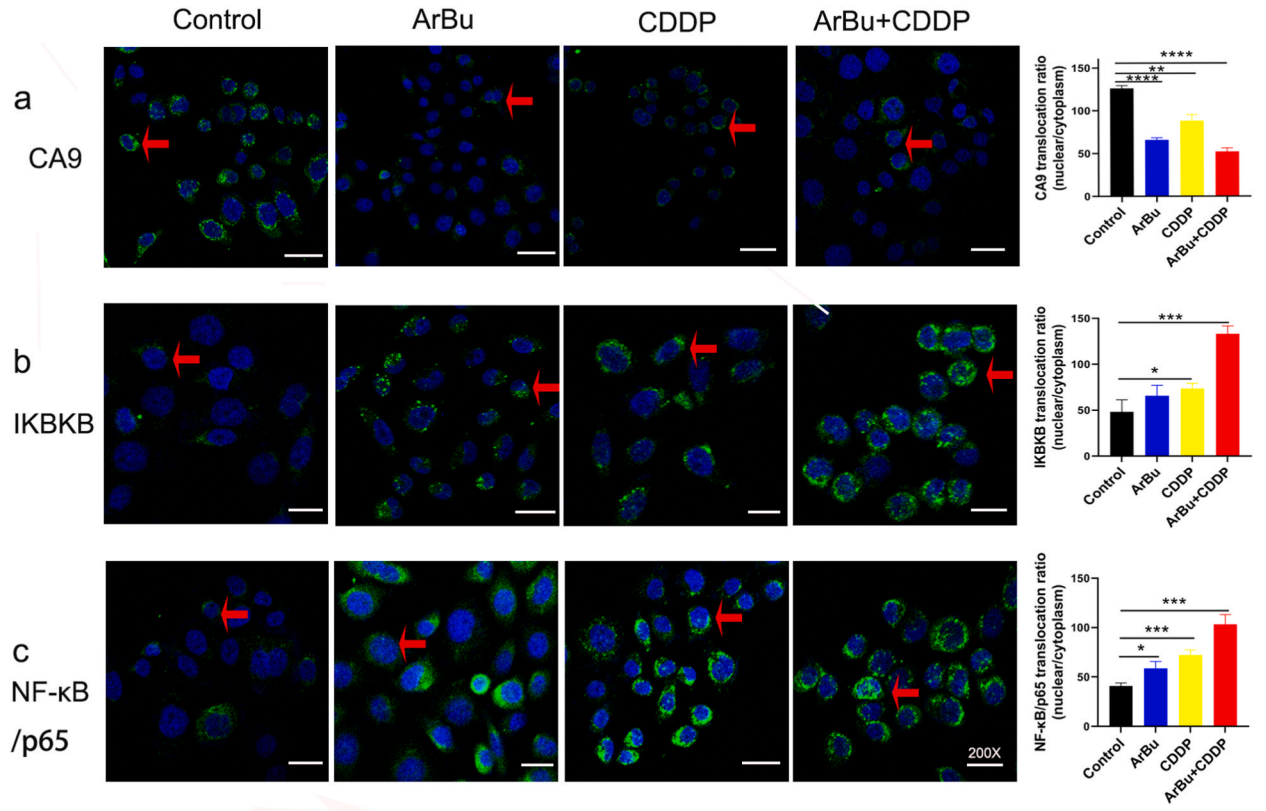

Fig. 5. Alkaliptosis-related proteins were detected by immunofluorescence staining (a, b, c) The localization of CA9, IKBKB, and NF-κB/p65 in the cytoplasm and nucleus of gastric cancer AGS cells treated with the control group, ArBu group (40 nM), CDDP group (40 μM), and ArBu combination with CDDP group (24.61 nM plus 28.37 μM) for 24 h was detected by immunofluorescence staining, respectively. Images were representative results of 3 independent experiments (200X). Arrows mean the translocation of CA9/IKBKB/NF-κB/p65. The data were presented as the mean (SD) of three independent experiments. $^{*}P < 0.05$ and $^{**}P < 0.01$, significantly different compared with the control treatment.

4. Discussion

In this study, we demonstrated that ArBu in combination with CDDP inhibited the proliferation and migration and promoted the apoptosis of gastric cancer cells in vitro as well as in a xenograft mouse model of gastric cancer by significantly regressing tumor growth compared to ArBu and CDDP treatment alone. In addition, the combination treatment down-regulated the expression of CA9 and up-regulated the expression of IKBKB and NF-κB/p65, suggesting that the synergistic effect was accompanied by the activation of the alkaliptosis pathway.

To our knowledge, this is the first study to explore the effects of the combination of ArBu and CDDP on gastric cancer. Previous studies have shown that ArBu treatment promotes apoptosis in SW1990 and BxPC3 human pancreatic cancer cells by activating autophagy activity [22]. Our research showed that AGS and MKN-45 cells treated with CDDP alone induced apoptosis when stained with AV-FITC/PI for flow cytometry analysis, and this effect was augmented when combined with ArBu. These results are similar to those of a previous study that showed that tetrandrine increased the sensitivity of CDDP-resistant A549 cells to CDDP and promoted apoptosis by downregulating the expression of Bcl2 and upregulating the expression of Bax [24]. Epithelial-mesenchymal transition (EMT) is an important process in normal embryonic development and is the most common initial cause of tumor invasion and metastasis [25]. In this study, we observed that ArBu in combination with CDDP significantly inhibited the levels of MMP-2 and MMP-9 and increased the level of E-cadherin, thereby reducing the degradation of the extracellular matrix (ECM) and basement membrane, resulting in reduced invasiveness of gastric cancer cells. Chen et al. showed that ArBu exhibited the strongest EMT inhibitory activity among the five compounds (cinobufotalin, bufarenogin, arenobufagin, 19-oxocinobufotalin and 19-hydroxybufalin), and they also demonstrated that the 11β-hydroxyl and 12-carbonyl structure of ArBu was associated with antineoplastic activity [26]. Additionally, we found that the combination of ArBu and CDDP effectively inhibited the characteristics of gastric cancer, including migration, and induced cell cycle arrest, reflected by enhanced toxicity, delayed wound healing, and decreased proportion of G0/G1 cells but increased number of G2/M phase cells compared to the single drug group in AGS and MKN-45 cells. Deng et al. suggested that ArBu blocked the transition from the G2 to M phase of the cell cycle by inhibiting the activation of the CDK1-Cyclin B1 complex, and demonstrated that ArBu directly binds to DNA to trigger the DNA damage response in vitro [16]. These results suggest that ArBu could be a promising therapy for gastric cancer via a variety of mechanisms. In our study, we also suggested that ArBu

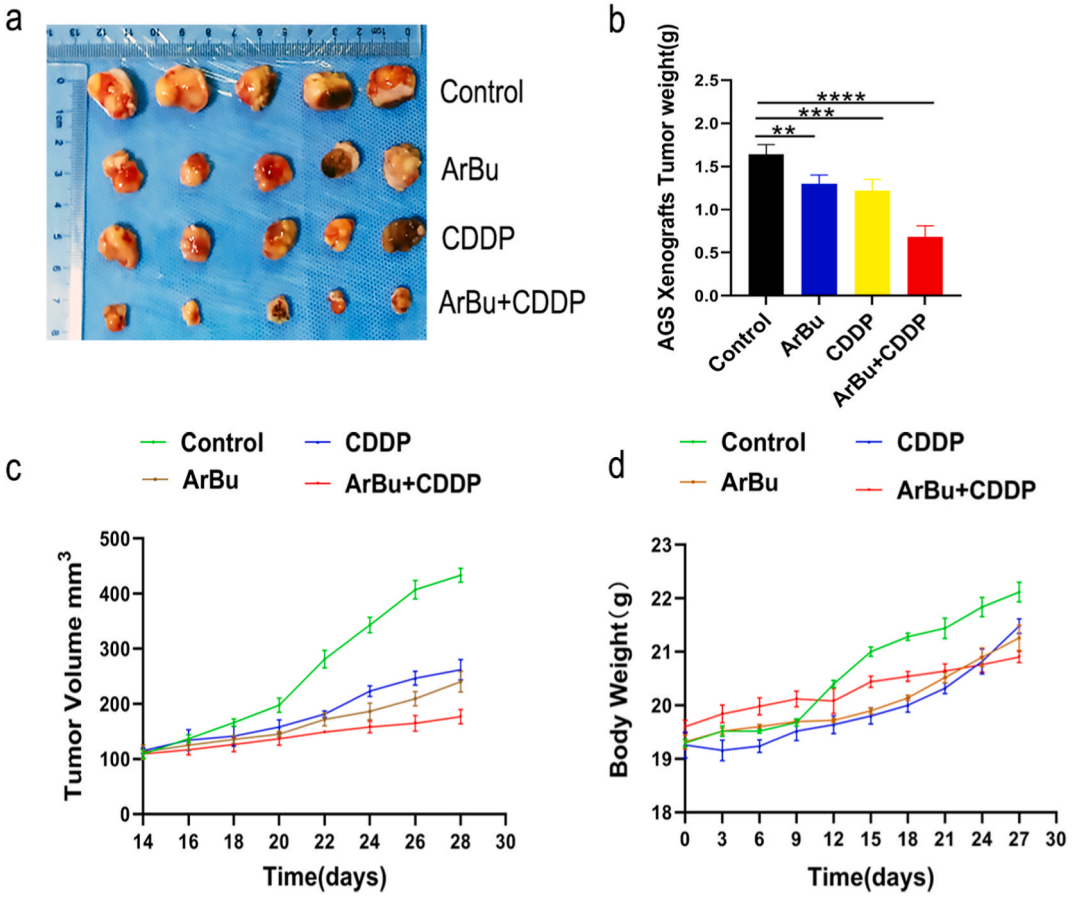

Fig. 6. ArBu combination with CDDP antitumor effect in vivo

Twenty nude mice were randomly divided into four groups, with five mice in each group. Nude mice bearing AGS xenograft tumors were treated with the control (0.1 % dimethylsulfoxide solvent control), ArBu group (6.4 mg/kg), CDDP (3 mg/kg), and ArBu in combination with CDDP group (6.4 mg/kg plus 3 mg/kg) for 24 days after subcutaneous inoculation of AGS cells in vivo. (a) Tumors were removed and photographed to observe changes in each group. (b) Tumor weight of each group. (c) Tumor volume of each group. (d) The mice body weight of each group. $*P < 0.05$ and $**P < 0.01$, significantly different compared with the control treatment.

treatment had antitumor activity in vivo and in vitro, and when ArBu synergized with CDDP, it could amplify the anticancer effect depending on the inhibition of invasion, migration, and proliferation through the activation of the alkaliptosis pathway.

Tumor cells mainly produce lactic acid and CO2 during anaerobic glycolysis, which promotes the formation of an acidic microenvironment and the overexpression of CA9 [27]. Furthermore, the expression of CA9 in hepatocellular carcinoma was negatively correlated with the expression of E-cadherin, which is associated with cell adhesion [18,28]. These suggest that alterations in the microenvironment are crucial for cell survival. Cell death is a basic mechanism that controls various physiological and pathological processes. Alkaliptosis, a pH-dependent form of regulated necrosis, is driven by intracellular alkalinization after IKBKB and NF-κB/p65 pathway-dependent downregulation of CA9, a protein which plays critical role in this process [29–31]. In the present study, we showed significantly lower expression of CA9 and higher expression of IKBKB and NF-κB/p65 in the ArBu combination with CDDP group than in the ArBu or CDDP groups, which demonstrated alkaliptosis pathway activation in human gastric cells. Moreover, we observed that the combination of ArBu and CDDP effectively reduced the tumor growth rate in a xenograft mouse model of gastric cancer, accompanied by alkaliptosis activation. Garbati et al. showed that CA9 expression in neuroblastoma nodules was strongly correlated with the growth rate of tumor masses and negatively correlated with their apoptotic rate; they also demonstrated that acetazolamide, a CA9 inhibitor combined with CDDP, could delay tumor growth rate and improve progression-free survival more strongly than CDDP or acetazolamide alone [32]. In our study, we detected lower levels of CA9, a key protein in the alkaliptosis process, in the ArBu combination with CDDP group than in the ArBu and CDDP groups. To our knowledge, the CA9 is usually over-expressed in several solid tumors, as a consequence, converts CO2 to HCO3− and H + [33]. In addition, we further detected the related proteins, IKBKB and NF-κB/p65 of alkaliptosis. Notably, the data reported here demonstrate the suitability of this hypothesis: the combination of ArBu and CDDP inhibited the CA9 level to delay the growth of gastric cancer by activating alkaliptosis, and the co-administration of ArBu significantly enhanced CDDP efficacy. Our study only confirmed that the antitumor effect of ArBu combined with CDDP is through the activation of the alkaliptosis pathway, but additional mechanisms, such as the interaction of drug structures,

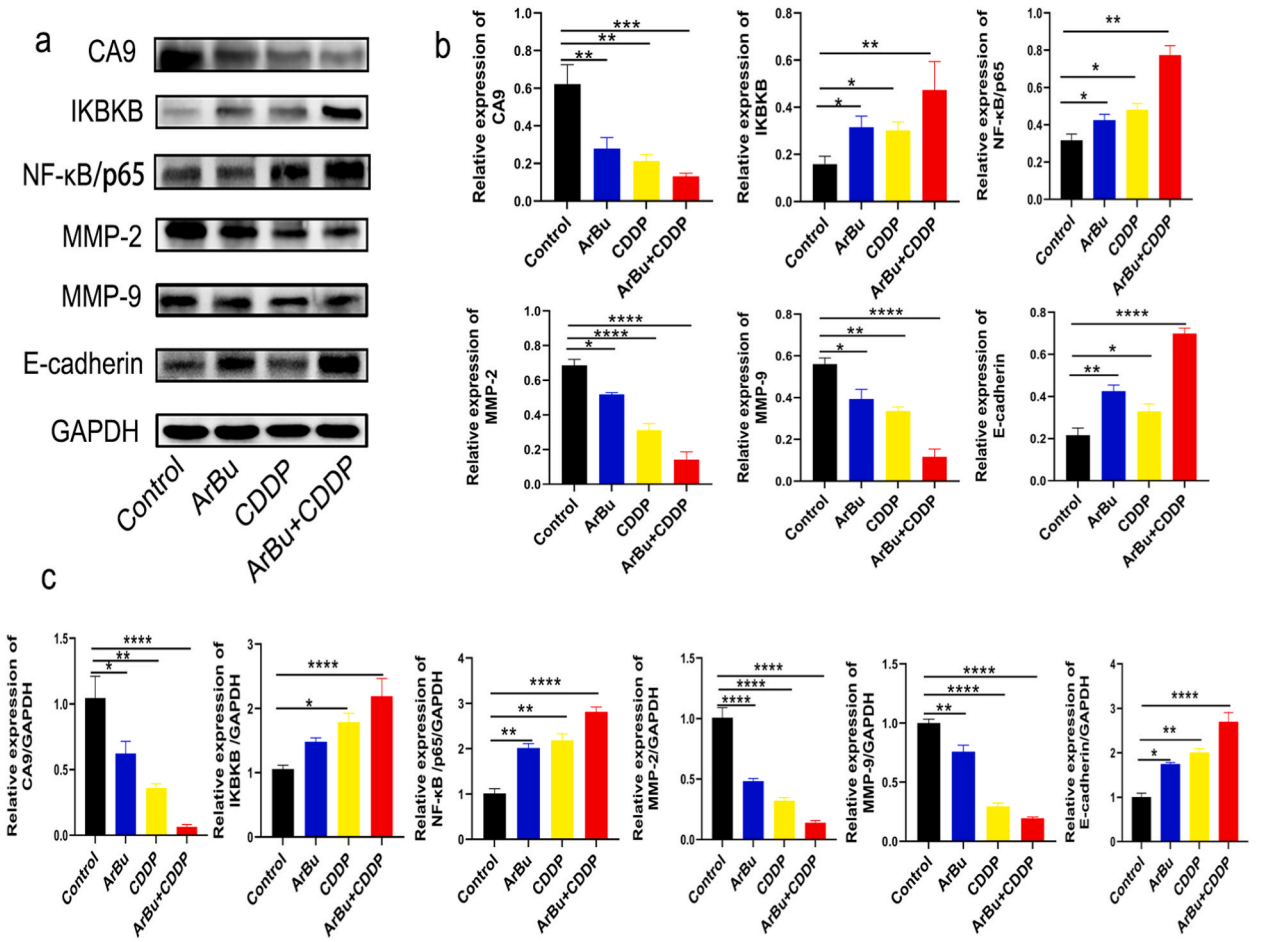

Fig. 7. The combination of ArBu and CDDP regulates alkaliptosis-related protein and mRNA expression in vivo (a, b) The protein expression of CA9, IKBKB, NF-κB/p65, MMP-2, MMP-9, E-cadherin, and GAPDH in AGS cells was estimated by western blotting. (c) The mRNA expression of CA9, IKBKB, NF-κB/p65, MMP-2, MMP-9, and E-cadherin in AGS cells. The mRNA level was detected by RT-PCR analysis. The data were presented as the mean (SD) of three independent experiments. $^{*}P < 0.05$ and $^{**}P < 0.01$, significantly different compared with the control treatment.

may exist, which is the direction and content of our further research.

In summary, the present study shows that ArBu enhances the inhibitory effect on the growth of gastric cancer cells, both in vitro and in vivo, when combined with CDDP. This effect was thought to be mediated by the alkaliptosis pathway. Our study provides a theoretical basis for the application of ArBu in combination with CDDP as a potent agent for gastric cancer treatment.

Ethics approval and consent to participate

The experimental protocol was established, according to the ethical guidelines of the.

Declaration of Helsinki and mouse experiments were approved by the Institutional Animal Care and Use Committee of the First Affiliated Hospital of Anhui Medical University (Approval Number: LLSC20180365) in accordance with the Guide for the Care and Use of Laboratory Animals.

Consent for publication

All authors have read and agreed to the published version of the manuscript.

Funding

This study was supported by the Anhui Provincial Natural Science Foundation (grant number: 1608085MH182).

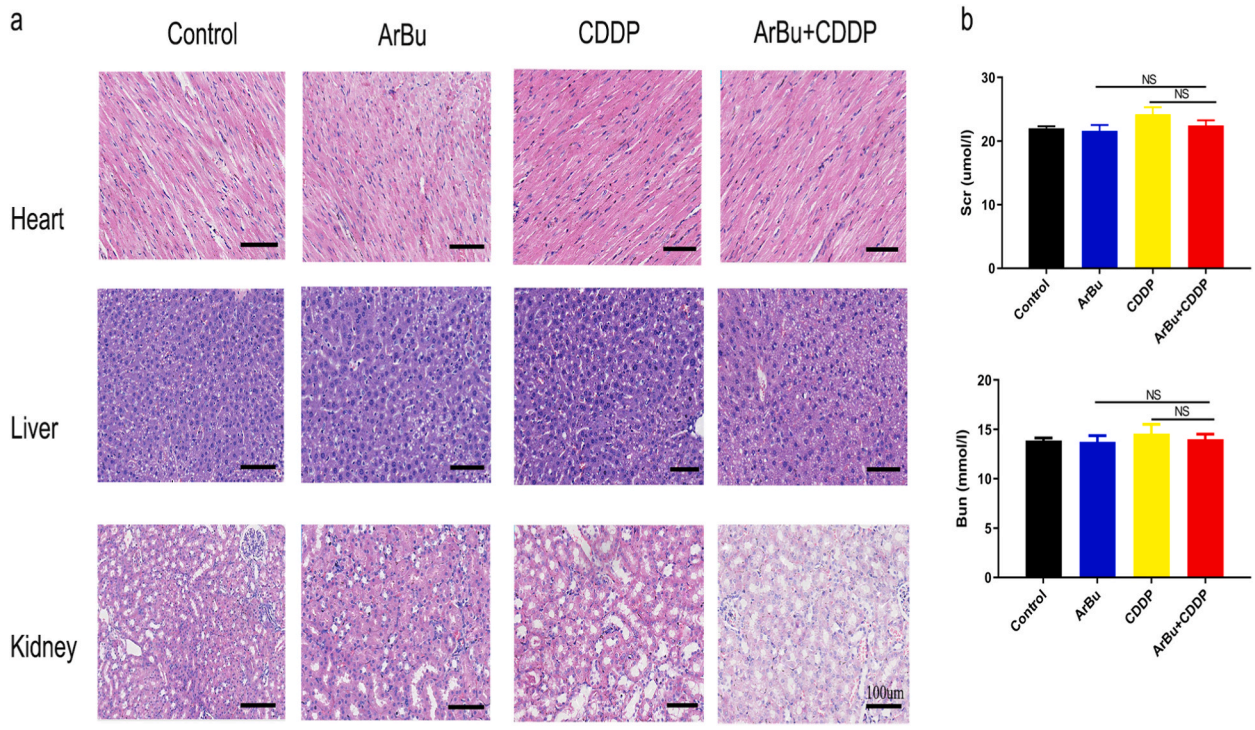

Fig. 8. Effect of ArBu combined with CDDP on organs in vivo (a) Pathological changes of the transplanted heart, liver, and kidney in each group (HE staining × 40 times). (b) Serum creatinine and blood urea nitrogen in the blood of mice. The data were presented as the mean (SD) of three independent experiments. NS means no significance.

Data availability statement

Data included in article/supp. Material/referenced in article.

CRediT authorship contribution statement

Chengwei Liu: Writing – review & editing, Writing – original draft, Data curation. **Dongchang Li:** Data curation. **Jian Wang:** Data curation. **Zhengguang Wang:** Writing – review & editing, Investigation, Funding acquisition, Conceptualization.

Declaration of competing interest

The authors declare that they have no known competing financial interests or personal relationships that could have appeared to influence the work reported in this paper.

Acknowledgements

We thank Hongwei Yao for guiding this manuscript.

Appendix A. Supplementary data

Supplementary data to this article can be found online at https://doi.org/10.1016/j.heliyon.2023.e21110.

References

[1] J.A. Ajani, et al., Gastric cancer, version 2.2022, NCCN clinical Practice guidelines in oncology, J. Natl. Compr. Cancer Netw. 20 (2) (2022) 167–192.
[2] U. Hacker, A. Hoffmeister, F. Lordick, [Gastric Cancer: diagnosis and current treatment strategies], Dtsch. Med. Wochenschr. 146 (23) (2021) 1533–1537.
[3] L. Yang, et al., The relative and attributable risks of cardia and non-cardia gastric cancer associated with Helicobacter pylori infection in China: a case-cohort study, Lancet Public Health 6 (12) (2021) e888–e896.
[4] K. Li, et al., Advances in clinical immunotherapy for gastric cancer, Biochim. Biophys. Acta Rev. Canc 1876 (2) (2021), 188615.

[5] D.H. Ilson, Advances in the treatment of gastric cancer: 2020-2021, Curr. Opin. Gastroenterol. 37 (6) (2021) 615–618.
[6] S. Ghosh, Cisplatin: the first metal based anticancer drug, Bioorg. Chem. 88 (2019), 102925.
[7] S. Dasari, P.B. Tchounwou, Cisplatin in cancer therapy: molecular mechanisms of action, Eur. J. Pharmacol. 740 (2014) 364–378.
[8] R.C. Kiss, F. Xia, S. Acklin, Targeting DNA damage response and repair to enhance therapeutic index in cisplatin-based cancer treatment, Int. J. Mol. Sci. 22 (15) (2021).
[9] R. Siegel, et al., Cancer treatment and survivorship statistics, 2012, Ca - Cancer J. Clin. 62 (4) (2012) 220–241.
[10] J.S. Liu, et al., Anti-tumor effects and 3D-quantitative structure-activity relationship analysis of bufadienolides from toad venom, Fitoterapia 134 (2019) 362–371.
[11] L. Soumoy, et al., Bufalin for an innovative therapeutic approach against cancer, Pharmacol. Res. 184 (2022), 106442.
[12] J. Zhao, et al., Arenobufagin, isolated from toad venom, inhibited epithelial-to-mesenchymal transition and suppressed migration and invasion of lung cancer cells via targeting IKKβ/NFκB signal cascade, J. Ethnopharmacol. 250 (2020), 112492.
[13] L.J. Deng, et al., 1β-OH-arenobufagin induces mitochondrial apoptosis in hepatocellular carcinoma through the suppression of mTOR signaling pathway, J. Ethnopharmacol. 266 (2021), 113443.
[14] Y. Zhang, et al., Cytotoxic effects of hellebrigenin and arenobufagin against human breast cancer cells, Front. Oncol. 11 (2021), 711220.
[15] D.M. Zhang, et al., Arenobufagin, a natural bufadienolide from toad venom, induces apoptosis and autophagy in human hepatocellular carcinoma cells through inhibition of PI3K/Akt/mTOR pathway, Carcinogenesis 34 (6) (2013) 1331–1342.
[16] L.J. Deng, et al., Arenobufagin intercalates with DNA leading to G2 cell cycle arrest via ATM/ATR pathway, Oncotarget 6 (33) (2015) 34258–34275.
[17] J. Liu, et al., Alkaliptosis: a new weapon for cancer therapy, Cancer Gene Ther. 27 (5) (2020) 267–269.
[18] S. Hyuga, et al., Expression of carbonic anhydrase IX is associated with poor prognosis through regulation of the epithelial-mesenchymal transition in hepatocellular carcinoma, Int. J. Oncol. 51 (4) (2017) 1179–1190.
[19] A. Giatromanolaki, et al., Expression of hypoxia-inducible carbonic anhydrase-9 relates to angiogenic pathways and independently to poor outcome in non-small cell lung cancer, Cancer Res. 61 (21) (2001) 7992–7998.
[20] Z. Li, et al., Carbonic anhydrase 9 confers resistance to ferroptosis/apoptosis in malignant mesothelioma under hypoxia, Redox Biol. 26 (2019), 101297.
[21] J.L. Bryant, et al., Novel carbonic anhydrase IX-targeted therapy enhances the anti-tumour effects of cisplatin in small cell lung cancer, Int. J. Cancer 142 (1) (2018) 191–201.
[22] X. Wei, et al., Arenobufagin inhibits the phosphatidylinositol 3-kinase/Protein kinase B/mammalian target of rapamycin pathway and induces apoptosis and autophagy in pancreatic cancer cells, Pancreas 49 (2) (2020) 261–272.
[23] Y. Kurman, et al., Cucurbitacin B and cisplatin induce the cell death pathways in MB49 mouse bladder cancer model, Exp. Biol. Med. 245 (9) (2020) 805–814.
[24] L.Y. Ye, et al., The effect of tetrandrine combined with cisplatin on proliferation and apoptosis of A549/DDP cells and A549 cells, Cancer Cell Int. 17 (2017) 40.
[25] I. Pastushenko, C. Blanpain, EMT transition states during tumor progression and metastasis, Trends Cell Biol. 29 (3) (2019) 212–226.
[26] L. Chen, et al., Arenobufagin inhibits prostate cancer epithelial-mesenchymal transition and metastasis by down-regulating β-catenin, Pharmacol. Res. 123 (2017) 130–142.
[27] J.X. Wang, et al., Lactic acid and an acidic tumor microenvironment suppress anticancer immunity, Int. J. Mol. Sci. 21 (21) (2020).
[28] S.J. Yu, et al., Inhibition of hypoxia-inducible carbonic anhydrase-IX enhances hexokinase II inhibitor-induced hepatocellular carcinoma cell apoptosis, Acta Pharmacol. Sin. 32 (7) (2011) 912–920.
[29] M. Benej, S. Pastorekova, J. Pastorek, Carbonic anhydrase IX: regulation and role in cancer, Subcell. Biochem. 75 (2014) 199–219.
[30] H.M. Becker, Carbonic anhydrase IX and acid transport in cancer, Br. J. Cancer 122 (2) (2020) 157–167.
[31] X. Song, et al., JTC801 induces pH-dependent death specifically in cancer cells and slows growth of tumors in mice, Gastroenterology 154 (5) (2018) 1480–1493.
[32] P. Garbati, et al., MCM2 and carbonic anhydrase 9 are novel potential targets for neuroblastoma pharmacological treatment, Biomedicines 8 (11) (2020).
[33] G. Venkateswaran, S. Dedhar, Interplay of carbonic anhydrase IX with amino acid and acid/base transporters in the hypoxic tumor microenvironment, Front. Cell Dev. Biol. 8 (2020), 602668.